THE JOURNAL OF BIOLOGICAL CHEMISTRY VOL. 287, NO. 21, pp. 17353–17362, May 18, 2012

Endothelin Induces Rapid, Dynamin-mediated Budding of Endothelial Caveolae Rich in ET-B*[S]

Received for publication, January 3, 2012, and in revised form, March 27, 2012 Published, JBC Papers in Press, March 28, 2012, DOI 10.1074/jbc.M111.338897

Phil Oh, Thierry Horner, Halina Witkiewicz, and Jan E. Schnitzer[1]

From the Proteogenomics Research Institute for Systems Medicine, San Diego, California 92121

Background: Whether physiological ligands can regulate caveolae trafficking in endothelial cells is unknown.
Results: ET-B is concentrated in endothelial caveolae. Endothelins are very potent stimulators of rapid dynamin-mediated internalization of caveolae and their cargo in endothelial cells *in vitro* and under native conditions in tissue.
Conclusion: Caveolae can mediate rapid endocytosis when induced by select GPCR ligands.
Significance: We reveal a new function for endothelin in regulated caveolae trafficking in endothelial cells.

Clathrin-independent trafficking pathways for internalizing G protein-coupled receptors (GPCRs) remain undefined. Clathrin-mediated endocytosis of receptors including ligand-engaged GPCRs can be very rapid and comprehensive (<10 min). Caveolae-mediated endocytosis of ligands and antibodies has been reported to be much slower in cell culture (≫10 min). Little is known about the role of physiological ligands and specific GPCRs in regulating caveolae trafficking. Here, we find that one receptor for endothelin, ET-B but not ET-A, resides on endothelial cell surfaces in both tissue and cell culture primarily concentrated within caveolae. Reconstituted cell-free budding assays show that endothelins (ETs) induce the fission of caveolae from endothelial plasma membranes purified from rat lungs. Electron microcopy of lung tissue sections and tissue subcellular fractionation both show that endothelin administered intravascularly in rats also induces a significant loss of caveolae at the luminal surface of lung vascular endothelium. Endothelial cells in culture show that ET stimulates very rapid internalization of caveolae and cargo including caveolin, caveolae-targeting antibody, and itself. The ET-B inhibitor BQ788, but not the ET-A inhibitor BQ123, blocks the ET-induced budding of caveolae. Both the pharmacological inhibitor Dynasore and the genetic dominant negative K44A mutant of dynamin prevent this induced budding and internalization of caveolae. Also shRNA lentivirus knockdown of caveolin-1 expression prevents rapid internalization of ET and ET-B. It appears that endothelin can engage ET-B already highly concentrated in caveolae of endothelial cells to induce very rapid caveolae fission and endocytosis. This transport requires active dynamin function. Caveolae trafficking may occur more rapidly than previously documented when it is stimulated by a specific ligand to signaling receptors already located in caveolae before ligand engagement.

Caveolae are flask-shaped plasmalemmal invaginations in many cell types that endocytose select toxins (1–3), viruses (4), and conformationally modified proteins (5). In vascular endothelial cells lining the blood vessels of specific organs where they are especially abundant, caveolae also transport select blood-borne macromolecules and even specific targeting antibodies across this formidable cell barrier to reach cells inside the tissue (5–7). Caveolar budding or fission from the plasma membrane to form free vesicles requires dynamin-mediated GTP hydrolysis at the caveolar neck (3, 8, 9).

The dynamics of caveolar internalization are currently unclear. Internalization of SV40 virus and sequestered cell surface proteins (*i.e.* glycosylphosphatidylinositol-anchored proteins) can be mediated by caveolae via a relatively slow process taking 1–2 h (4, 10). It has even been reported that caveolae are static (11) and do not engage in constitutive vesicular trafficking (12). However, at least in endothelial cells *in vitro*, caveolae can endocytose select molecules within 20–30 min (5, 7, 9, 13). Select proteins and antibodies, usually linked to gold nanoparticles, can be transcytosed within 15 min (6). Until recently this trafficking pathway generally appeared to traffic more slowly than clathrin-dependent endocytic pathways. Dynamic imaging using intravital fluorescence video microscopy demonstrated *in vivo* that caveolae transcytosis can be very rapid (14). After intravenous injection, only antibodies targeting proteins constitutively residing within caveolae are transported across lung vascular endothelium and into the lung tissue within seconds of binding. Within minutes of intravenous injection, the whole lung tissue is flooded with antibody percolating through the lung interstitium. This very rapid transvascular transport occurs against a substantial concentration gradient and therefore is by definition active transport or pumping (14). Physiological ligands that bind their receptors already concentrated within caveolae for rapid trafficking into and/or across the endothelium are unknown.

Clathrin-coated vesicles can mediate the internalization of many GPCRs,[2] a process that is important for receptor desensitization and possible signaling within the cell (15, 16).

* This work was supported, in whole or in part, by National Institutes of Health Grants HL52766, HL58216, and HL67386.
[S] This article contains supplemental Figs. S1 and S2.
[1] To whom correspondence should be addressed: Proteogenomics Research Institute for Systems Medicine, 11107 Roselle St., San Diego, CA. Tel.: 858-450-9999; Fax: 858-450-9888; E-mail: jschnitzer@prism-sd.org.

[2] The abbreviations used are: GPCR, G protein-coupled receptor; ET, endothelin; ACE, angiotensin-converting enzyme; P, luminal endothelial cell plasma membranes; V, caveolae of P; RLMVEC, rat lung microvascular endothelial cell(s); BAEC, bovine aortic endothelial cell(s); eGFP, enhanced GFP; shCav1, shRNA lentiviral transduction particle to caveolin-1; cav1, caveolin-1; 5′NT, 5′-nucleotidase.

Although it appears quite clear that clathrin-independent pathways for GPCR internalization exist (16, 17), alternative pathways have yet to be well defined. Caveolin-GPCR interactions have been reported along with caveolin-dependent GPCR internalization; however, the caveolin binding motif has been mapped to the extracellular portion of the GPCR not likely to facilitate interaction with caveolin (18–21), which extends into, but not across, the lipid membrane. Although select GPCR and key signaling molecules may exist in caveolae and/or lipid rafts (22), their internalization by caveolae as well as their role in regulating caveolae budding and endocytosis remain substantially undefined. GPCR may sequester in caveolae and/or lipid rafts after ligand engagement (23–26). It is also unclear whether ligand-induced budding can occur without sequestration via receptors already localized a priori in caveolae. Physiological GPCR ligands that induce rapid endocytosis comparable with the clathrin pathway have yet to be identified for caveolae.

Endothelins (ETs) are endogenous ligands that play a key role in vascular homeostasis. They are among the most potent vasoconstrictors known and have been implicated in vascular diseases of several organ systems, including hypertension (27). Two endothelin receptor subtypes exist, endothelin receptor type A (ET-A) and type B (ET-B). In the vasculature, ET-A and ET-B are expressed in vascular smooth muscle cells to mediate vasoconstriction (28, 29). ET-B is also expressed in endothelial cells, where it functions to remove ET from the circulation (30–32). Upon stimulation, both receptor types undergo internalization for signal termination or possibly, signal persistence (15, 33, 34). Both ET-A and ET-B can be endocytosed through clathrin-coated pits (33, 34), but ET-A has also been found in caveolin-rich fractions from smooth muscle cells (35). ET-B is internalized and sorted into the late endosomal/lysosomal pathway, unlike ET-A, which is recycled (33, 34). The effects of ET on endothelial cells and how it is processed by endothelial cells remain unclear.

Here, to begin to assess the role of caveolae in internalization of ligand-engaged receptors, we used our *in vitro*, reconstituted, cell-free budding assay for caveolae to screen for ligands that can directly induce the fission of caveolae from endothelial cell plasma membranes. We identify ETs as very potent stimulators of caveolae budding via ET-B, which are already concentrated in caveolae before ligand engagement. We then confirm that this novel function for ET occurs in intact cells by showing that ET induces very rapid internalization of caveolae and its contents in endothelial cells in cell culture, as well as under native conditions in tissue.

EXPERIMENTAL PROCEDURES

Materials—The following materials were used: endothelin-1 (ET-1), -2, and -3 (Sigma or Peninsula Laboratories, San Carlos, CA); BQ123 and BQ788 (EMD Biosciences, Philadelphia, PA); ATP, GTP, Dynasore, and shRNA lentiviral transduction particle to caveolin-1 (cav1) (clone ID TRCN0000008002) and control shRNA (Sigma-Aldrich); antibodies to caveolin-1 and -2 and transferrin receptor (rabbit polyclonal and mouse monoclonal #Z034; BD Biosciences, San Diego, CA and rabbit polyclonal; Santa Cruz Biotechnology, Santa Cruz, CA); antibodies to angiotensin-converting enzyme (ACE) (Santa Cruz Biotechnology); tetramethylrhodamine-conjugated ET-1 and Tfn (iron-saturated) and biotin-conjugated ET-1 (Phoenix Pharmaceuticals, Burlingame, CA); antibodies to clathrin (BD Biosciences); antibodies to β-actin and albumin (Sigma); Texas Red anti-rabbit IgG, BODIPY anti-mouse IgG, Alexa 568 anti-rabbit IgG, and Alexa 488 anti-rabbit IgG (Invitrogen); HRP-conjugated anti-mouse or anti-rabbit IgG secondary antibodies and streptavidin (GE Healthcare); antibodies to ET-B (Dr. Miyoung Chun, Boston University School of Medicine); antibodies to 5′-nucleotidase (5′NT) (Dr. Paul Luzio, University of Cambridge); monoclonal antibodies mAPP2 (aminopeptidase P2, a mAb to a caveolar protein) and TX3.406 (generated in-house); rat lung microvascular endothelial cells (RLMVEC; Dr. Karen Guice University, North Carolina, Chapel Hill); bovine aortic endothelial cells (BAEC; Ken Baker, Sandoz, Boston, MA); caveolin-1-eGFP expression construct (Dr. Giusy Fiucci, ORT, Paris, France); wild type dynamin2- and K44A dynamin2-eGFP expression constructs (Dr. Mark McNiven, Mayo Clinic); Eps15-eGFP (mutant Eps15 delta 95–295) (Dr. Frances Brodsky, UCSF); and tetramethylbenzidine liquid substrate system for ELISA (Sigma-Aldrich; St. Louis, MO).

Isolation of Luminal Endothelial Cell Plasma Membranes and Caveolae—The luminal endothelial cell plasma membranes (P) and their caveolae (V) were isolated directly from rat lung tissue using an *in situ* silica coating procedure as described (9, 13, 22, 36–40).

Western Analysis—Proteins from the tissue subfractions were solubilized with cell lysis buffer (2 M urea, 0.5 M Tris, pH 6.8, 3 mM EDTA, 3% SDS), separated by SDS-PAGE, and transferred to nitrocellulose filters for immunoblotting with the appropriate antibodies as described (14, 36, 38, 41).

ET-1 Treatment of Rat Lungs in Situ—The lungs of male Sprague-Dawley rats were perfused at 37 °C via the pulmonary artery as described (36). Briefly, the lungs were flushed with mammalian Ringer's solution at constant pressure (8 mm Hg) prior to perfusion with either Ringer's solution or ET-1 in Ringer's for 2 min and then allowed to stand for 3 min (for total ET-1 incubation time of 5 min). The lungs were then flushed with MES buffered saline, pH 6, for 1.5 min at 4 °C followed by silica perfusion and processing to isolate silica-coated luminal endothelial cell plasma membranes as described (9, 13, 22, 36–40).

In Vitro Caveolar Fission Assay—As described in our past work (3), a cell-free assay for caveolar fission was reconstituted with the silica-coated luminal endothelial cell plasma membranes (P) purified from rat lung. Briefly, P (20 μg) were incubated for 30 min at 37 °C with calf brain cytosol (1 mg/ml) 2 mM ATP, 30 μM GTP (3) plus ETs (as indicated). In some cases, P were preincubated at 37 °C with cytosol from HeLa cells expressing either wild type or K44A mutant dynamin for 60 min (replacing brain cytosol in assay). Sucrose was added to a final concentration of 40% in 20 mM KCl, layered with 0–35% continuous sucrose gradient, and then subjected to centrifugation for 4 h at 50,000 rpm (TLA50 rotor in a Beckman Ultramax centrifuge) at 4 °C (3). The membrane pellet (P-V_b) was processed for Western analysis as described (9). The extent of budding was quantified followed by densitometry to measure loss of caveolin signal from the membrane pellet. In some cases, the floating, budded caveolae (V_b) were collected and tested for

specific proteins of interest by Western analysis. For the collection of $V_{b,}$ 100 μg of P was used.

Immunofluorescence Microscopy—RLMVEC, human umbilical vein endothelial cells, and BAEC were grown on coverslips for dual immunofluorescence confocal microscopy as described in our past work (9). The cells were incubated with TX3.406 (1 μg/ml) and/or antibodies to 5′NT (1 μg/ml) at 4 °C for 30 min to label cell surface caveolae or lipid rafts, respectively. The cells were fixed and permeabilized with methanol at −20 °C, blocked with 2% goat serum, and then stained with caveolin-1 (1:1000) or ET-B (1:100) antibodies. For ET-B and clathrin, the cells were fixed prior to labeling with antibodies to ET-B (1:100), clathrin (1:500), and/or caveolin-1 (1:500). The bound primary antibody was detected with a reporter IgG conjugated to Texas Red (anti-rabbit IgG) or BODIPY (anti-mouse IgG). The immunofluorescence signal was visualized and photographed using a confocal fluorescence microscope (Perkin Elmer Wallac, Gaithersburg, MD).

ET-1-induced Internalization of Caveolae—BAEC or RLMVEC were transiently transfected to express caveolin-1 fused to eGFP, Eps15 mutant fused to eGFP, wild type, or K44A Dynamin2 fused to eGFP using Lipofectamine 2000 following the manufacturer's protocol. Alternatively, BAEC were infected for 24 h with shRNA lentiviral transduction particle to caveolin-1 (shCav1) following the manufacturer's protocol.

Fluorescenated probes, ET-1 or Tfn, were bound to the cell surface at 4 °C for 1 h. The cells were then warmed to 37 °C for 5 min followed by fixation with 2% paraformadehyde, permeabilization with 1% Triton X-100, and incubation with primary antibody followed by appropriate fluorophore-conjugated reporter antibody. Alternatively, TX406 or 5′NT antibody was bound at 4 °C prior to ET-1 addition and incubation at 37 °C, fixation with 2% paraformadehyde, permeabilization with 1% Triton X-100, and labeling with a fluorophore-conjugated reporter. In some experiments, the cells were treated with ET-1, fixed, and permeabilized as above before labeling with the primary antibody(s) to ET-B and/or cav1 followed by fluorophore-conjugated reporter as described above for dual immunofluorescence microscopy. The cells were visualized using confocal fluorescence microscopy.

Enzyme-linked Avidin-based Detection Assay for Cell Surface ET-1—BAEC were plated onto a 96-well plate and allowed to grow until confluent. In some cases, cells were infected for 24 h with either caveolin-1 (shCav1) or a control shRNA lentiviral transduction particle following the manufacturer's protocol. Biotinylated ET-1 was bound to intact, nonfixed cells at 4 °C for 1 h. Some cells were immediately fixed, but not permeabilized, with 2% paraformadehyde followed by labeling with HRP-conjugated streptavidin and signal development using tetramethylbenzidine substrate following manufacturer's protocol. Other cells were warmed to 37 °C for 5 min before processing as above.

Electron Microscopy—The lungs of male Sprague-Dawley rats were perfused with ET-1 or vehicle control and allowed to incubate for 5 min. The lungs were then flushed with MES buffered saline, pH 6, for 1.5 min at 4 °C, fixed by perfusion with 30 ml of 4% paraformaldehyde, 0.1% glutaraldehyde in 0.1 M sodium cacodylate, pH 7.4, and excised. The tissue was cut into ~1-mm^3 pieces, incubated for 2 h at 4 °C in the same fixative, washed with 0.1 M sodium cacodylate-HCl buffer, pH 7.4 (three times for 15 min each time), and post-fixed for 60 min on ice in 1% OsO_4 in 0.1 M sodium cacodylate buffer, pH 7.0. The fixed specimens were then processed through dehydration and embedding in Epon. The embedded blocks were cut into sections, stained with lead and uranyl acetate by standard procedures as in our past work (9, 36), and analyzed using a FEI Morgani 268D transmission electron microscope with a CCD camera system for EM digital imaging. Caveolar density at the cell surface was quantified by morphometric analysis of randomly selected fields (range of sample size was 15–76 fields) as described in our past work (9, 36).

RESULTS

Ligand Stimulation of Caveolar Budding—We tested the direct and immediate effects of various compounds on the budding of caveolae using a reconstituted cell-free assay that focuses only on the last steps of the budding process, namely fission, of the caveolae as described previously (3, 9). Briefly, we incubated silica-coated P isolated from rat lungs (36) with reconstituted cytosol supplemented with ET-1, insulin, mastoparan analog (MAS7), VEGF, or albumin, before separating any budded caveolae from the plasma membranes by centrifugation (3). The loss of cav1 signal from the membrane pellet was measured by Western analysis to quantify caveolar budding (3). Only the heterotrimeric G protein activators, ET-1 and MAS7, induced caveolar fission (data not shown). Looking for direct effectors of caveolae fission from plasma membranes, we found that a well known physiological ligand ET-1 can stimulate endothelial caveolar budding.

To characterize ET-1-induced caveolar fission in more detail, we varied the ET-1 concentration and the incubation time in our *in vitro* assay. At all time points tested, ET-1 with 30 μM GTP in the cytosol stimulated caveolar budding (Fig. 1*A*) as indicated by the reduced signal for cav1. The level of ET-induced budding appeared comparable with the maximal response detected in this assay for 1 mM GTP alone (Fig. 1*B*) as described previously (3). This caveolar fission was maximally induced at ET-1 doses of ≥30 nM. ET-B was also released from the endothelial cell plasma membranes in a dose-dependent manner and to a similar extent as cav1. Conversely, cell surface marker proteins not concentrated in caveolae, such as ACE, remained constant (also true for the cytoskeletal marker, β-actin, as well as lipid raft marker, 5′NT (data not shown)). We also observed similar induction with ET-2 and ET-3 (Fig. 1*C* and data not shown). Thus, endothelins stimulated the fission of caveolae from the plasma membrane in a time- and dose-dependent manner. The concentration profile of ET-1 inducing caveolar fission is consistent with past experiments studying ET receptor interactions and signaling in cultured cells (17, 33, 42–44). Base on these data, we used ET1 at 30–100 nM for the studies described below.

Although it is well known that endothelial cells primarily express ET-B and not ET-A and although we could not detect ET-A by Western analysis in the isolated endothelial cell membranes (data not shown), we still decided to assess the specific function of ET-B in this process by using pharmacological

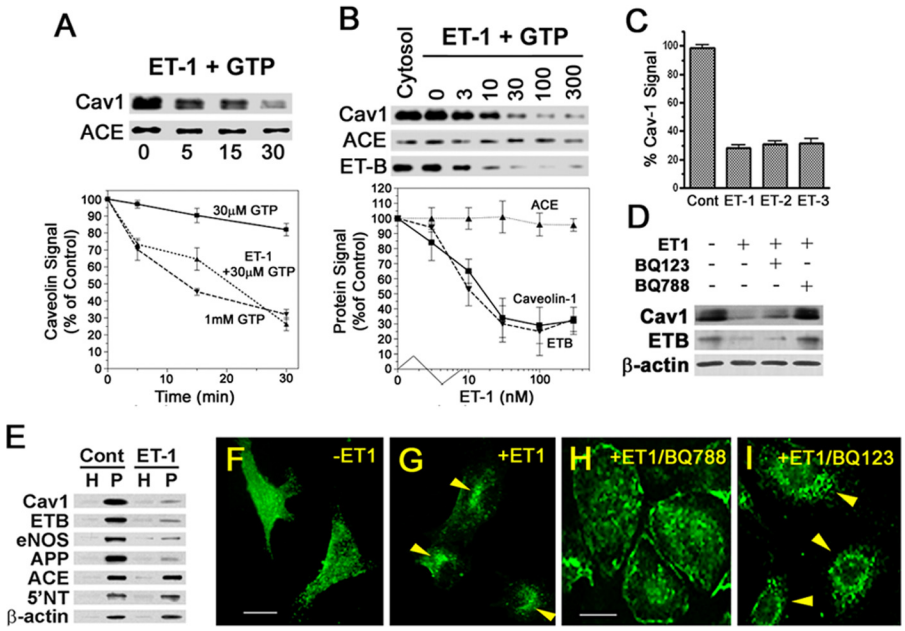

FIGURE 1. **Endothelins induce endothelial caveolae budding *in vitro*, in cell culture, and *in situ*.** *A–D*, *in vitro* reconstituted cell-free budding assay (see "Experimental Procedures"). Western blot analysis of repelleted silica-coated endothelial plasma membranes showing the signal for the indicated proteins either after 100 nM ET-1 stimulation for the indicated times (*A*) or stimulation with indicated concentration (nM) of ET-1 for 30 min (*B*). The graphs represent the quantified signal from the Western blot analysis as a percentage of control signal (either ET-1 at time 0 or no ET-1, respectively) for the indicated protein and then plotted as a function of incubation time (*A*) or ET-1 concentration (*B*). *C*, histogram showing relative cav1 signal remaining on repelleted silica-coated endothelial plasma membranes after 30 min of treatment with of ET-1, ET-2, and ET-3. *D*, Western blot analysis of the repelleted silica-coated endothelial plasma membrane proteins showing the signal for the indicated primary antibodies after 30 min of pretreatment with either 50 nM BQ123 (ET-A antagonist) or 5 nM BQ788 (ET-B antagonist) followed by 30 min of stimulation with ET-1. *E*, Western blot analysis of silica-coated endothelial plasma membranes isolated from rat lungs showing the signal for the indicated primary antibodies after 5 min of stimulation with ET-1. *F–I*, confocal fluorescence microscopic images of cav1-eGFP expressing BAEC showing caveolin-1 localization either untreated (*F*) or after 5 min of stimulation with ET-1 (*G*). Confocal fluorescence microscopic images of BAEC showing localization of caveolin-1 after pretreated for 30 min with either 5 nM BQ788 (*H*) or 50 nM BQ123 (*I*) followed by 5 min of stimulation with ET-1. The *arrowheads* indicate cav1 perinuclear intracellular localization. *H*, total lung homogenate; *eNOS*, endothelial nitric-oxide synthase. *Cont*, control. All of the graphs are the percentages of the control cav1 signal detected without ET1 exposure. $n \geq 3$ experiments. The *bar* represents 100 μm.

antagonist specific to either ET-A (BQ123) or ET-B (BQ788). Using our *in vitro* caveolae fission assay, BQ788 but not BQ123 inhibited the ability of ET to induce caveolae fission (Fig. 1*D*). These data are consistent with the involvement of ET-B and not ET-A in ET-induced caveolae budding.

ET-1 Stimulates Caveolae Budding in Endothelial Cells in Tissue—To determine whether ET-1 stimulates the budding of caveolae natively in vascular endothelium in tissue, we perfused the rat lung microvasculature with ET-1 or control vehicle. After 5 min of exposure, we flushed the lungs and isolated their P for comparative Western analysis (Fig. 1*E*). ET-1 caused a >70% decrease (when compared with vehicle control) in cav1 and APP2 (a lung endothelial caveolae marker protein (14)), whereas the ACE and 5′NT levels remained unchanged.

We also performed electron microscopy with morphometric analysis on tissue sections from the ET-1-perfused rat lungs. ET-1 caused a significant decrease ($p < 0.001$) in caveolar density in pulmonary microvessels (1.00 ± 0.31 caveola/μm linear luminal endothelial cell surface membrane in ET-1-stimulated lungs *versus* 1.84 ± 0.52 caveolae/μm membrane in unstimulated rats). We similarly detected ET-1-induced budding of caveolae in endothelial cells of the descending aorta (data not shown). Thus, ET-1 also stimulated caveolar budding in intact endothelial cells growing under physiologically and native conditions in tissue.

ET1-induced Caveolin Internalization in Cultured Endothelial Cells—We used fluorescence imaging to assess ET-1-induced internalization of caveolae by transfecting BAEC to express caveolin-EGFP fusion protein (cav1-eGFP) to mark the caveolae. These cells were incubated or not with ET-1 and then imaged using fluorescence confocal microscopy. Within minutes of exposure to ET-1, there was a clear and significant redistribution of the cav1-eGFP from the cell surface into the cell. By 10 min, large intracellular punctae were readily apparent in virtually all of the cells (Fig. 1*F*). This extensive and rapid internalization of caveolae and redistribution of caveolin was not detected without ET-1 stimulation (Fig. 1*G*). Again BQ788 (Fig. 1*H*) but not BQ123 (Fig. 1*I*) prevented this induction of caveolae budding, resulting here in no redistribution of caveolin. Our data so far are consistent with ET-1 inducing caveolar budding from the plasma membrane very rapidly via a mechanism requiring specific engagement and activation of ET-B.

ET-B Localizes to Dynamic Caveolae—Various GPCR, such as BkR, appear to require ligand engagement to sequester apparently in caveolae and/or lipid rafts (23–26). To determine whether the receptor for endothelin in endothelial cells, ET-B, resides on its own already concentrated in caveolae, we performed Western analysis on subcellular fractions of rat lung tissue. cav1 and ET-B were highly enriched in P *versus* the total tissue homogenate and even more enriched in the isolated V over P (Fig. 2*A*). V was also enriched in other EM-validated

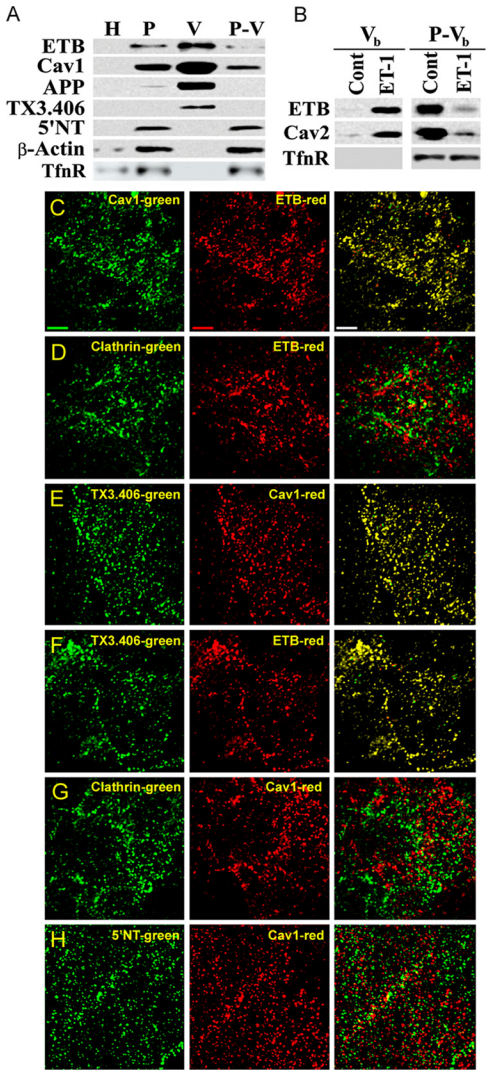

FIGURE 2. **ET-B is concentrated specifically in dynamic caveolae capable of budding to form free transport vesicles.** *A*, Western blot analysis of subcellular fractions (1 μg) isolated from rat lung tissue (see "Experimental Procedures"). *H*, whole lung homogenates; *P-V*, repelleted silica-coated membranes stripped of caveolae. *B*, Western blot analysis of caveolae induced to bud by ET-1 in the *in vitro* reconstituted budding assay (see "Experimental Procedures"). P either untreated (control, *Cont*) or treated with ET-1 for 30 min at 37 °C was subjected to sucrose density centrifugation to separate the low density caveolae vesicles released from P (V_b) from the repelleted silica-coated endothelial plasma membrane proteins (P-V_b). *C–H*, dual immunofluorescence microscopy of intact RLMVEC incubated at 4 °C with antibodies (see "Experimental Procedures") as indicated. Single channel *green* and *red* fluorescence images are shown along with the merged images with both signals. Colocalization of signals generates *yellow* in the overlay of the two images. *Bar*, 2 μm. *TfnR*, transferrin receptor; *Cav2*, caveolin-2.

caveolar antigens such as APP2. As reported previously (36, 45), V was markedly depleted in the lipid raft marker 5′NT as well as the cytoskeletal protein β-actin. The clathrin vesicle marker transferrin receptor (Fig. 2*A*) and clathrin heavy chain (data not shown) were detected in P but not V; they actually remained in the repelleted membrane fraction after removing caveolae (P-V). As reported previously (10, 22, 36, 38, 45–47), this isolation technique separates caveolae from lipid rafts and isolates endothelial cell surface caveolae from lung tissue to >95% purity.

Some caveolae may possibly be static structures (12). To address whether ET-B resides in dynamic caveolae capable of budding from the endothelial cell surface to form free transport vesicles, we again performed the reconstituted cell-free budding assay but focused this time on the free caveolae budded away from the repelleted plasma membrane. We incubated P with ET-1 to stimulate caveolar fission before separating and isolating by flotation any budded caveolae (V_b) from the rest of the repelleted membrane (P-V_b). With ET-1-induced caveolae fission, ET-B and caveolin were found to be quite enriched in V_b and depleted in P-V_b (Fig. 2*B* and data not shown). Conversely, a protein found in clathrin-coated vesicles, transferrin receptor, had little to no signal found in V_b, and its signal seemed to remain unchanged in P-V_b in the presence or absence of ET-1. Thus, ET-B remain concentrated in the dynamic caveolae that have been induced to bud by ET-1 and that are isolated independently of clathrin-coated vesicles.

To investigate further the cell surface localization of ET-B, we performed dual immunofluorescence microscopy on cultured RLMVEC. Consistent with past reports (9, 22, 37), cav1 antibodies revealed a punctate staining pattern marking the caveolae on the cell surface (Fig. 2, *C* and *F–H*). ET-B (Fig. 2, *C–E*) and the antibody TX3.406 (Fig. 2, *E* and *F*) also displayed punctate cell surface staining, indicating their elevated concentration within discrete plasmalemmal microdomains. When the images were overlaid, both ET-B and TX3.406 showed significant colocalization with cav1 (Fig. 2, *C* and *F*, *yellow signal*), as well as each other (Fig. 2*E*). Conversely, the staining for the glycosylphosphatidylinositol-anchored lipid raft protein, 5′NT, was also found to be punctate, yet this microdomain showed little overlap with cav1 (Fig. 2*H*). Similarly, the staining for clathrin was punctate without overlapping with either cav1 or ET-B (Fig. 2, *D* and *G*). Thus, both subcellular fractionation isolates yielding caveolae (mechanically dislodged and physiologically budded) and immunofluorescence microscopy of intact endothelial cells revealed that ET-B resides at the endothelial cell surface already quite concentrated in dynamic caveolae distinct from other cell surface microdomains such as lipid rafts and clathrin-coated pits. This compartmentalization appears to exist for endothelial cells in tissue and in cell culture. ET-B engagement by ET-1 induced the fission of caveolae from the plasma membrane to form free vesicles rich in cav1 and ET-B.

ET-1-induced Fission of Caveolae Requires GTPase-competent Dynamin—The GTPase dynamin can mediate caveolae fission, and the dominant negative mutant dynamin can inhibit caveolae budding (3, 8, 9). To investigate whether ET-1-induced caveolar budding is dynamin-dependent, we performed the *in vitro* caveolar fission assay on P using cytosol containing wild type dynamin or the K44A dynamin, a dominant negative mutant that poorly hydrolyzes GTP (Fig. 3*A*). Using several markers (cav1, TX3.406, and APP2) previously shown to be concentrated within caveolae (41, 45, 48, 49) (Fig. 2, *A* and *F*),[3] we found that ET-1 reduced the signal for these proteins as well as ET-B in the presence of wild type dynamin but not mutant dynamin. Conversely, ACE and 5′NT remained in the membrane pellet regardless of stimulation by ET-1 or very high GTP concentrations (1 mM).

[3] P. Oh and J. E. Schnitzer, personal observation.

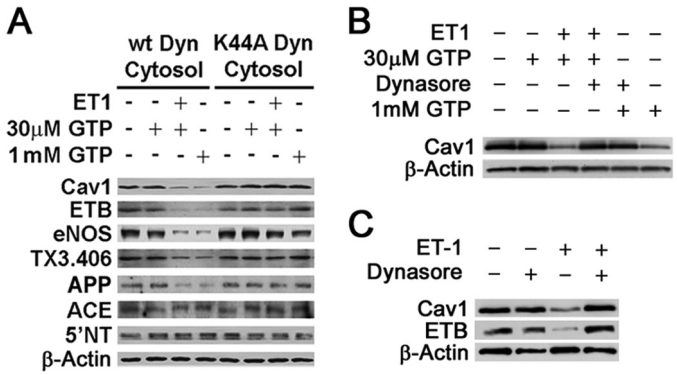

FIGURE 3. **Role of dynamin in caveolae fission induced by ET-1.** *A*, Western blot analysis of repelleted endothelial cell plasma membranes after performing the *in vitro* reconstituted budding assay in the presence of ET-1 for 30 min, GTP, and either wild type (*wt*) or K44A mutant dynamin containing cytosol as indicated (see "Experimental Procedures"). *B*, same as *A* but used standard cytosol and as indicated with 50 μM Dynasore (30 min of pretreatment before ET-1 and also included with ET-1). *C*, Western analysis of silica-coated endothelial plasma membranes isolated from rat lungs that had been treated *in situ* (see "Experimental Procedures") with ET-1 and/or 50 μM Dynasore. Dynasore was administered for 10 min and then also combined with ET-1 as indicated.

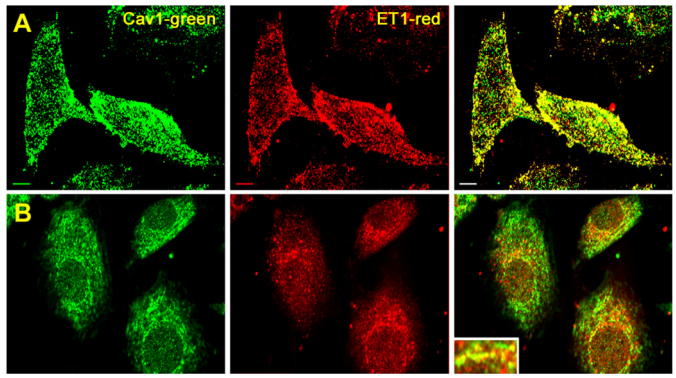

FIGURE 4. **ET-1 is rapidly internalized by caveolae in cultured endothelial cells.** Images from confocal fluorescence microscopy of tetramethylrhodamine-ET1 localization (*red*) on intact BAEC immediately fixed after 4 °C binding (*A*) or after the cells were warmed to 37 °C for 5 min (*B*) prior to fixation with paraformadehyde. The cells were then permeabilized before incubation with cav1 antibodies and fluorophore-conjugated reporter antibodies (cav1, *green*). The *bar* represents 50 μm.

To assess further the role of dynamin in ET-1-induced caveolar fission, we used a pharmacological inhibitor of dynamin, Dynasore (50, 51). To confirm for the first time that Dynasore could inhibit caveolar fission and thus was functionally quite similar to the dominant negative mutant K44A dynamin, we performed our *in vitro* reconstituted cell-free budding assay. Dynasore was preincubated in cytosol containing normal dynamin prior to incubation with P and ET-1 stimulation as described above. Again there was little to no observable ET-1 induced caveolar budding when dynamin was inhibited (Fig. 3*B*). Thus, both pharmacological and genetic means of inhibition showed the critical role of dynamin in endothelin-induced caveolae fission.

We extended these *in vitro* studies to evaluating dynamin's function in intact endothelial cells in lung tissue by simply including Dynasore with ET administered intravascularly in rats. Western analysis again showed that ET-1 within minutes was able to induce substantial budding of caveolae rich in ET-B as measured by loss of caveolin and ET-B signal in P isolated from the lung tissue (Fig. 3*C*). Dynasore completely inhibited this effect of endothelin. Thus, ET specifically induced caveolar fission in reconstituted cell-free assay *in vitro* and in intact endothelial cells in lung tissue via a dynamin-dependent mechanism.

ET-1 Internalization in Cultured Endothelial Cells—We used ET-1 conjugated to tetramethylrhodamine to follow the cell surface dynamics and internalization of ET-1 and cav1 simultaneously in intact cells. At 4 °C, ET-1 and cav1 colocalize significantly on the cell surface. Some cells showed >70% colocalization (Fig. 4*A*), whereas others exhibited 30% colocalization. ET-1 was rapidly internalized within minutes after warm up to 37 °C (Fig. 4*B*). Most of the ET-1 at the cell surface appeared to move inside the cell within 10 min to produce strong intracellular punctate staining. Dominant negative mutant dynamin prevented this endocytosis when we performed the same experimental protocol this time using BAEC transiently transfected with K44A dynamin2 fused to eGFP. The cells expressing K44A dynamin2-eGFP lacked any intracellular accumulation of ET-1 (Fig. 5, *A* and *B*). However, the neighboring cells not expressing K44A dynamin2-eGFP still showed ample intracellular perinuclear punctate staining of the ET-1 probe (Fig. 5, *A* and *B*, *outlined cell*). Similarly induced expression of another dominant negative mutant protein, Eps15 mutant, an inhibitor of clathrin-mediated endocytosis (52), did not prevent rapid ET-1 (Fig. 5, *C* and *D*, *arrowheads*), yet expression of this Eps15 mutant did inhibit transferrin internalization (Fig. 5, *E* and *F*, *arrowhead*), and thus the mutant form was active. In other experiments, we followed ET-B internalization after ET-1 stimulation of the cells. Again, K44A dynamin (supplemental Fig. S1*A*) but not Eps15 mutant (supplemental Fig. S1*B*) prevented internalization in this case of the ET-1 receptor ETB. Thus, the internalization of ET-1 and its receptor ET-B via caveolae in cultured endothelial cells is dependent on active dynamin.

In these experiments, we did have some concern with the ET-1-tetramethylrhodamine probe in part because of our inability to compete much of its cell surface binding with naked ET-1 not conjugated to a fluorophore. The hydrophobicity of the fluorophore attached to such a small molecule may cause direct lipid membrane interaction. Regardless, our data here are still consistent with rapid dynamin-mediated endocytosis of ET-1 by caveolae and not by clathrin-coated vesicles. However, better fluorescent ET probes are needed because this probe may lack the desired specificity for ET-B and thus caveolae. Hence, we did not pursue further studies with this probe. It appears that with ET-B already concentrated in caveolae, ET can rapidly stimulate dynamin-mediated fission of caveolae that drives internalization of caveolae and its cargo into the cell.

ET-1 and ET-B Internalization Requires Caveolin-1—To assess the role for caveolin in ET endocytosis and whether caveolae are indeed required for this internalization, we inhibited cav1 expression in BAEC using shRNA lentiviral transduction particle specific for cav1. Routinely we were able to reduce caveolin-1 expression by >75–80% (supplemental Fig. S2). Upon ET-1 treatment of control cells expressing caveolin-1, we observed rapid ETB endocytosis as well as ET-B and caveolin-1

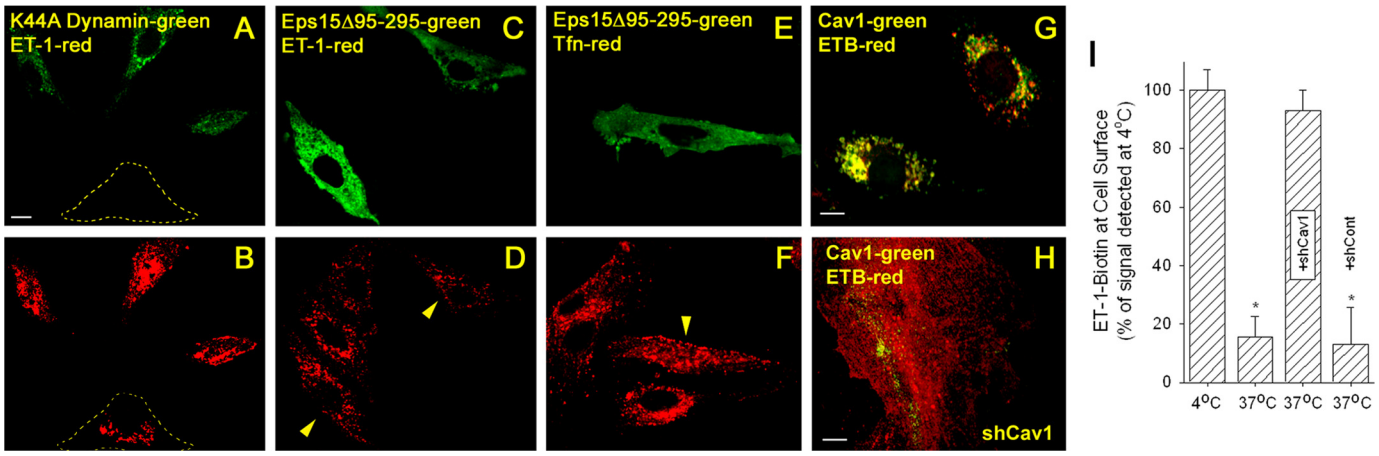

FIGURE 5. **Role of dynamin and caveolin-1 but not Eps15 in rapid internalization of ET-1 and ET-B in cultured endothelial cells.** *A–F*, images from confocal fluorescence microscopy of intact BAEC expressing either K44A Dynamin2-eGFP (*green*) (*A* and *B*) or Eps15-eGFP mutant (*green*) (*C–F*), and localization of either tetramethylrhodamine-ET1 (*red*) (*A–D*) or tetramethylrhodamine-Tfn (*red*) (*E* and *F*) after binding at 4 °C followed by warming to 37 °C for 5 min prior to fixation with paraformaldehyde (see "Experimental Procedures"). The *dashed lines* in *A* and *B* outline the positions of untransfected cell. The *arrowheads* in *D* and *F* denote Eps15 mutant transfected cells. *G* and *H*, localization of cav1 and ETB after 5 min of stimulation with ET1 of BAEC that were uninfected (*G*) or already infected for 24 h with shCav1 (*H*). *I*, histogram showing relative biotinylated ET-1 cell surface signal detected using an enzyme-linked, avidin-based detection assay (see "Experimental Procedures"). Intact, nonfixed BAEC were incubated with biotinylated ET-1 at 4 °C. Some cells (labeled *4* °C) were immediately fixed and processed for biotin detection. The other cells (labeled *37* °C) were first warmed to 37 °C for 5 min before processing. The cells infected for 24 h with shRNA lentivirus transduction particle are indicated as either +shCav1 for caveolin-1 shRNA or with control shRNA lentivirus transduction particle (+*shCont*) for control shRNA. *, $p < 0.05$ (analysis of variance/Tukey's range test). $n \geq 3$ experiments of triplicate wells for each experiment. The *bar* represents 50 μm.

intracellular perinuclear colocalization (Fig. 5*G*), but in cells showing minimal to no detectable caveolin-1 expression, we observed little to no intracellular perinuclear signal and only cell surface signal for ET-B (Fig. 5*H*). We also performed a warm-up internalization experiment using biotinylated-ET-1 and an enzyme-linked, avidin-based detection assay to confirm that ET-1 remained at the cell surface after cav1 knockdown (Fig. 5*I*). With 5 min of warming of the cells at 37 °C, the ET-1 surface signal decreased by >80% both in the uninfected cells, as well as cells infected with a control shRNA lentivirus transduction particle (shCont). ET remained completely detectable at the cell surface when the cells were kept at 4 °C as well as when the cells were infected with shCav1. Thus, cav1 and caveolae are necessary for rapid internalization of ET-1 and ET-B.

ET-1 Induces the Internalization of TX3.406, a Caveolar Targeting Antibody—To determine further whether the ET-induced, dynamin-dependent endocytosis was restricted to caveolae and to avoid possible off target interactions of the ET-fluorophore, we also evaluated the effect of ET-1 on endocytosis in intact, untransfected cultured cells by using two antibody probes: 5′NT, which targets lipid rafts, and TX3.406, which targets caveolae from outside the cell. As discussed earlier, Fig. 2 (*E* and *F*) shows excellent colocalization with caveolin-1 and ET-B at the cell surface when TX3.406 was incubated with endothelial cells at 4 °C. In these new experiments, TX3.406 and 5′NT antibodies were allowed to bind the surface of RLMVEC at 4 °C prior to warming to 37 °C in the presence or absence of ET-1. Within 5 min of warming, only the ET-1-exposed cells showed extensive internalization of TX3.406, which rapidly concentrated in discrete vesicular structures seen as large punctate signals inside the cells (Fig. 6, *A–D*). These large intracellular vesicles still contained cav1 (Fig. 6*D*). By comparison, the antibody to 5′NT remained at the cell surface in the absence or presence of ET-1 (Fig. 6, *E* and *F*). Consistent

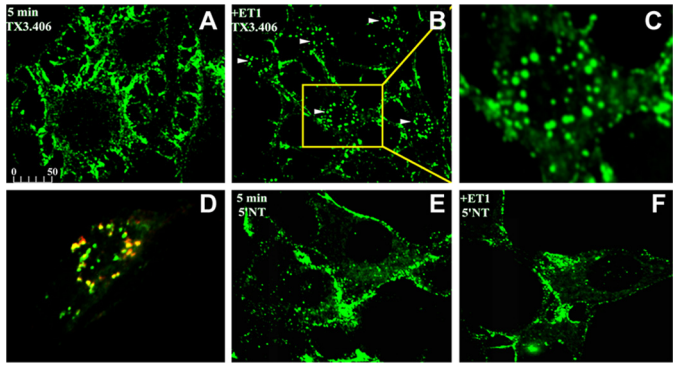

FIGURE 6. **ET-1-induced internalization of TX3.406, an antibody targeting caveolae, in cultured cells.** Images from confocal fluorescence microscopy of intact RLMVEC incubated at 4 °C with either TX3.406 (*A–D*) or 5′NT antibody (*E* and *F*) to label caveolae and lipid rafts, respectively. The cells were then incubated for 5 min at 37 °C in the presence (*B–D* and *F*) or absence (*A* and *E*) of ET-1 and then fixed and processed with fluorescent reporter antibody (*green*). *C*, magnified image of cell indicated by *arrow* and *yellow box* in *B*. *D*, the RLMVEC stimulated with ET-1 were also permeabilized and incubated with polyclonal antibody to caveolin-1 followed by fluorescent reporter antibody to rabbit IgG (*red*). The *arrowheads* indicate internalized signal. The *bar* represents 50 μm (*A*, *B*, and *D–F*) or 10 μm (*C*).

with these results, TX3.406 but not 5′NT antibodies became quite resistant to trypsin digestion within 5 min (data not shown). This induction of rapid internalization of the caveolae probe parallels our findings in BAEC using cav1-eGFP as a marker of caveolae (Fig. 1, *F* and *G*).

We also performed the same experimental protocol using RLMVEC transiently transfected with wild type normal dynamin2-eGFP and mutant K44Adynamin2-eGFP (Fig. 7). Cells expressing wild type dynamin2-eGFP, as well as nearby cells not effectively transfected, showed intracellular perinuclear TX3.406 accumulation (indicated by *arrowheads*) (Fig. 7*B*). The cells expressing K44A dynamin2-eGFP did not, despite neighboring cells (indicated by *arrowheads*) not

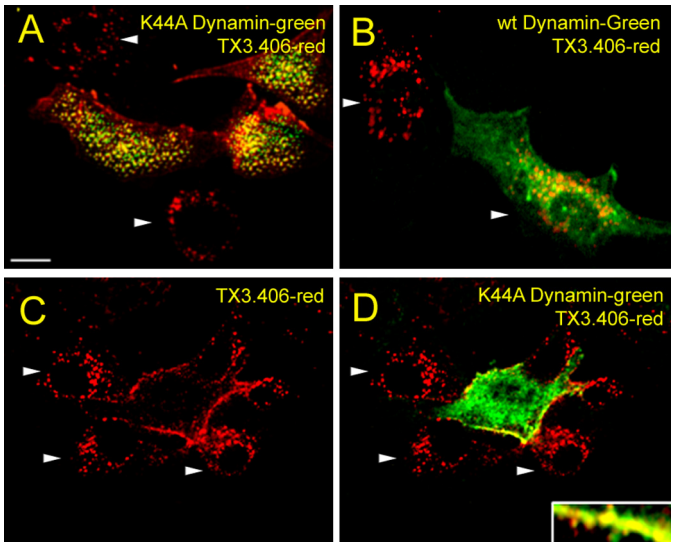

FIGURE 7. **Role of dynamin in ET-1 induced internalization of TX3.406 in cultured endothelial cells.** Images from confocal fluorescence microscopy of RLMVEC already transfected to express either K44A dynamin2-eGFP (*green*) (*A*, *C*, and *D*) or wild type (*wt*) dynamin2-eGFP (*green*) (*B*). The cells were incubated with TX3.406 for 1 h at 4 °C and washed before 5 min of stimulation with ET-1 at 37 °C and then fixation, permeabilization, and incubation with secondary fluorescent reporter antibody to mouse IgG (*red*). The *arrowheads* indicated intracellular perinuclear staining. *Bar*, 10 μm.

expressing K44A dynamin2-eGFP still showing caveolae internalization of the probe as indicated by the intracellular perinuclear punctate staining (Fig. 7, *A*, *C*, and *D*). Thus, ET-1 induces the rapid dynamin-mediated endocytosis of caveolae but not lipid rafts to form large cav1-containing intracellular vesicles.

DISCUSSION

Receptor-mediated endocytosis plays an important role in many physiological processes including GPCR signaling and sequestration (53). Caveolae and clathrin-coated pits are plasmalemmal vesicles that pinch off from the cell surface in a dynamin-dependent manner to internalize their cargo for intracellular sorting and trafficking (54). Although the role of clathrin-coated pits in GPCR internalization has been well characterized, it is becoming apparent that upon ligand engagement, many GPCR are rapidly internalized by other endocytic pathways not yet fully defined (17, 34, 35). Claing *et al.* (17) detected three distinct pathways for GPCR internalization. Pathway I (β_1 adrenergic receptor, β_2 adrenergic receptor, μ-opioid receptor, adenosine 2B receptor, and M1 muscarinic receptor) is inhibited by overexpressed mutant β-arrestin, K44A dynamin, and wild type small G protein-coupled receptor kinase-interacting protein, GIT1. Pathway II internalizes ET-B and vasoactive intestinal peptide 1 receptor and is inhibited by K44A dynamin but not by GIT1 or mutant β-arrestin. Pathway III (angiotensin 1A receptor and M2 muscarinic receptor) is not affected by overexpression of these three proteins. Clathrin vesicles clearly mediate Pathway I, but the endocytic mechanism for the others are unknown, although it has been speculated that caveolae mediate pathway II (17).

In this report, we use three different systems (an *in vitro* caveolae fission assay, intact cultured endothelial cells, and endothelial cells existing natively in tissue) to show conclusively that endothelins stimulates the dynamic internalization of caveolae rich in ET-B through a fission process requiring dynamin. Both Dynasore and the dominant negative mutant of dynamin, K44A, prevent caveolar budding induced by ET. Although ET-B internalization can be mediated in other cell types by clathrin-coated pits (34), we find, in endothelial cells, no evidence of clathrin colocalization with ET-B nor clathrin-mediated endocytosis of ET-1 or ET-B (no inhibition with dominant negative EPS-15). Endothelin induces the internalization of caveolae and its cargo in endothelial cells in culture and in tissue.

Unlike ET-B, which we show in endothelial cells resides already concentrated in caveolae that can respond directly and thus very quickly to ligand engagement, various GPCR such as bradykinin receptors appear to first require ligand engagement for sequestration into caveolae and/or lipid rafts, possibly for delayed, slow internalization (19, 23–26, 55). These studies are mostly based on overexpressing transfected cells and/or biochemical subfractionation techniques that are known to coisolate noncaveolar microdomains from the plasma membrane (*i.e.* lipid rafts) and even from intracellular compartments (*i.e.* Golgi and nuclei) (36, 45). Here, we show using lung tissue to avoid possible cell culture artifacts and using subcellular fractionation techniques that isolate caveolae separately from other detergent-resistant microdomains (*i.e.* lipid rafts) (3, 9, 36, 38, 45), that ET-B resides constitutively in caveolae rather than sequestering there only after ligand engagement. This finding is confirmed in intact cultured endothelial cells by confocal fluorescence microscopy showing ET-B signal as punctae that colocalize extensively with markers for caveolae but not markers for lipid rafts or clathrin-coated vesicles.

It is now apparent that caveolae can mediate very rapid internalization of select ligands. ET-B is localized and concentrated in caveolae of microvascular endothelial cells in rat lung as well as bovine aortic endothelial cells and rat lung microvascular endothelial cells. ET-1 can induce fission of caveolae in a reconstituted cell-free budding assay from endothelial cell plasma membranes purified from lungs and can stimulate the budding and internalization of caveolae in cultured endothelial cells. The budding and internalization of caveolae with ET-1 engagement of its receptor is very rapid. Caveolae are indeed dynamic structures capable of stimulated membrane trafficking. Here we discover that the natural physiological ligand, ET, can greatly speed up caveolae budding and internalization. Thus, caveolae may not be the slow endocytic pathway as envisioned previously (4–7, 9–13), but in fact their internalization may be tightly regulated and quite rapid after ligand engagement of specific receptors. Prepackaging the receptors in caveolae before ligand engagement likely eliminates time lost to sequestering receptors and probably is key to inducing very rapid endocytosis. This rapid internalization of ligand and receptor is likely important in the regulation of signal transduction either through homologous desensitization and/or delivery to specific internal compartments yet to be determined.

The rapid response in budding is also probably enabled by having dynamin as well as the rest of the ET-B signaling machinery (heterotrimeric G proteins and nonreceptor tyrosine kinases (22, 37)) already concentrated in caveolae before

ligand engagement. Dynamin is the key mechanical effector mediating end stage budding and is already polymerized like a spring around the neck of caveolae ready for immediate fission (9, 22, 37, 40). It is clear from the *in vitro* reconstituted cell-free assay, which focuses only on the last step of the caveolar budding process, namely fission, and not the invagination process or formation of new caveolae, that endothelin can directly stimulate caveolar fission. The polymeric ring of dynamin can generate the mechanical force and extension necessary to pinch off the mature caveolae from the plasma membrane to form free transport vesicles (3, 9, 56). It seems that caveolae can bud by first invaginating to form their mature, stable, omega-shaped structure and, at least in this case, by then waiting, poised and ready, for specific ligands to trigger their rapid, fission from the plasma membrane. This mechanism implies a role for caveolae beyond simple static signaling platforms toward acutely integrating or coupling receptor-mediated signaling to the internalization and trafficking of cell surface molecules and ligands. Thus, key signaling and trafficking molecules may indeed be concentrated *a priori* in caveolae to mediate very rapid responses to ligand engagement, resulting in rapid budding of caveolae. Although the regulated caveolae trafficking revealed in this study is likely fundamental to the biology of the cell, the exact signaling mechanisms and patho-physiological ramifications remain to be determined for this newly discovered biological process where a specific ligand can induce very rapid caveolae budding and internalization in endothelial cells.

Acknowledgments—We thank Drs. Miyoung Chun and Paul Luzio for the kind gifts of antibodies to ET-B and 5′NT; Drs. Mark McNiven, Frances Brodsky, and Giussy Fiucci for the kind gifts of constructs to dyn2GFP (wild type and K44A), Eps15-eGFP mutant, and cav1-eGFP; and Drs. Karen Guice and Ken Baker for the kind gifts of the endothelial cells RLMVEC and BAEC, respectively.

REFERENCES

1. Montesano, R., Roth, J., Robert, A., and Orci, L. (1982) Non-coated membrane invaginations are involved in binding and internalization of cholera and tetanus toxins. *Nature* **296,** 651–653
2. Parton, R. G., Joggerst, B., and Simons, K. (1994) Regulated internalization of caveolae. *J. Cell Biol.* **127,** 1199–1215
3. Schnitzer, J. E., Oh, P., and McIntosh, D. P. (1996) Role of GTP hydrolysis in fission of caveolae directly from plasma membranes. *Science* **274,** 239–242
4. Pelkmans, L., Kartenbeck, J., and Helenius, A. (2001) Caveolar endocytosis of simian virus 40 reveals a new two-step vesicular-transport pathway to the ER. *Nat. Cell Biol.* **3,** 473–483
5. Schnitzer, J. E., Oh, P., Pinney, E., and Allard, J. (1994) Filipin-sensitive caveolae-mediated transport in endothelium: reduced transcytosis, scavenger endocytosis, and capillary permeability of select macromolecules. *J. Cell Biol.* **127,** 1217–1232
6. McIntosh, D. P., Tan, X. Y., Oh, P., and Schnitzer, J. E. (2002) Targeting endothelium and its dynamic caveolae for tissue-specific transcytosis *in vivo*. A pathway to overcome cell barriers to drug and gene delivery. *Proc. Natl. Acad. Sci. U.S.A.* **99,** 1996–2001
7. Milici, A. J., Watrous, N. E., Stukenbrok, H., and Palade, G. E. (1987) Transcytosis of albumin in capillary endothelium. *J. Cell Biol.* **105,** 2603–2612
8. Henley, J. R., Krueger, E. W., Oswald, B. J., and McNiven, M. A. (1998) Dynamin-mediated internalization of caveolae. *J. Cell Biol.* **141,** 85–99
9. Oh, P., McIntosh, D. P., and Schnitzer, J. E. (1998) Dynamin at the neck of caveolae mediates their budding to form transport vesicles by GTP-driven fission from the plasma membrane of endothelium. *J. Cell Biol.* **141,** 101–114
10. Mayor, S., Rothberg, K. G., and Maxfield, F. R. (1994) Sequestration of GPI-anchored proteins in caveolae triggered by cross-linking. *Science* **264,** 1948–1951
11. Bundgaard, M. (1983) Vesicular transport in capillary endothelium. Does it occur? *Fed. Proc.* **42,** 2425–2430
12. Thomsen, P., Roepstorff, K., Stahlhut, M., and van Deurs, B. (2002) Caveolae are highly immobile plasma membrane microdomains, which are not involved in constitutive endocytic trafficking. *Mol. Biol. Cell* **13,** 238–250
13. McIntosh, D. P., and Schnitzer, J. E. (1999) Caveolae require intact VAMP for targeted transport in vascular endothelium. *Am. J. Physiol.* **277,** H2222–H2232
14. Oh, P., Borgström, P., Witkiewicz, H., Li, Y., Borgström, B. J., Chrastina, A., Iwata, K., Zinn, K. R., Baldwin, R., Testa, J. E., and Schnitzer, J. E. (2007) Live dynamic imaging of caveolae pumping targeted antibody rapidly and specifically across endothelium in the lung. *Nat. Biotechnol.* **25,** 327–337
15. Chun, M., Lin, H. Y., Henis, Y. I., and Lodish, H. F. (1995) Endothelin-induced endocytosis of cell surface ETA receptors. Endothelin remains intact and bound to the ETA receptor. *J. Biol. Chem.* **270,** 10855–10860
16. Ferguson, S. S. (2001) Evolving concepts in G protein-coupled receptor endocytosis. The role in receptor desensitization and signaling. *Pharmacol. Rev.* **53,** 1–24
17. Claing, A., Perry, S. J., Achiriloaie, M., Walker, J. K., Albanesi, J. P., Lefkowitz, R. J., and Premont, R. T. (2000) Multiple endocytic pathways of G protein-coupled receptors delineated by GIT1 sensitivity. *Proc. Natl. Acad. Sci. U.S.A.* **97,** 1119–1124
18. Ginés, S., Ciruela, F., Burgueño, J., Casadó, V., Canela, E. I., Mallol, J., Lluís, C., and Franco, R. (2001) Involvement of caveolin in ligand-induced recruitment and internalization of A(1) adenosine receptor and adenosine deaminase in an epithelial cell line. *Mol. Pharmacol.* **59,** 1314–1323
19. Igarashi, J., and Michel, T. (2000) Agonist-modulated targeting of the EDG-1 receptor to plasmalemmal caveolae. eNOS activation by sphingosine 1-phosphate and the role of caveolin-1 in sphingolipid signal transduction. *J. Biol. Chem.* **275,** 32363–32370
20. Schwencke, C., Okumura, S., Yamamoto, M., Geng, Y. J., and Ishikawa, Y. (1999) Colocalization of β-adrenergic receptors and caveolin within the plasma membrane. *J. Cell. Biochem.* **75,** 64–72
21. Yamaguchi, T., Murata, Y., Fujiyoshi, Y., and Doi, T. (2003) Regulated interaction of endothelin B receptor with caveolin-1. *Eur. J. Biochem.* **270,** 1816–1827
22. Oh, P., and Schnitzer, J. E. (2001) Segregation of heterotrimeric G proteins in cell surface microdomains. G_q binds caveolin to concentrate in caveolae, whereas G_i and G_s target lipid rafts by default. *Mol. Biol. Cell* **12,** 685–698
23. de Weerd, W. F., and Leeb-Lundberg, L. M. (1997) Bradykinin sequesters B2 bradykinin receptors and the receptor-coupled Galpha subunits $G\alpha_q$ and $G\alpha_i$ in caveolae in DDT1 MF-2 smooth muscle cells. *J. Biol. Chem.* **272,** 17858–17866
24. Haasemann, M., Cartaud, J., Muller-Esterl, W., and Dunia, I. (1998) Agonist-induced redistribution of bradykinin B2 receptor in caveolae. *J. Cell Sci.* **111,** 917–928
25. Feron, O., Han, X., and Kelly, R. A. (1999) Muscarinic cholinergic signaling in cardiac myocytes. Dynamic targeting of M2AChR to sarcolemmal caveolae and eNOS activation. *Life Sci.* **64,** 471–477
26. Ishizaka, N., Griendling, K. K., Lassègue, B., and Alexander, R. W. (1998) Angiotensin II type 1 receptor. Relationship with caveolae and caveolin after initial agonist stimulation. *Hypertension* **32,** 459–466
27. Agapitov, A. V., and Haynes, W. G. (2002) Role of endothelin in cardiovascular disease. *J. Renin Angiotensin Aldosterone Syst.* **3,** 1–15
28. Seo, B., Oemar, B. S., Siebenmann, R., von Segesser, L., and Lüscher, T. F. (1994) Both ETA and ETB receptors mediate contraction to endothelin-1 in human blood vessels. *Circulation* **89,** 1203–1208
29. Batra, V. K., McNeill, J. R., Xu, Y., Wilson, T. W., and Gopalakrishnan, V. (1993) ETB receptors on aortic smooth muscle cells of spontaneously hypertensive rats. *Am. J. Physiol.* **264,** C479–C484
30. Fukuroda, T., Fujikawa, T., Ozaki, S., Ishikawa, K., Yano, M., and Ni-

shikibe, M. (1994) Clearance of circulating endothelin-1 by ETB receptors in rats. *Biochem. Biophys. Res. Commun.* **199,** 1461–1465
31. de Nucci, G., Thomas, R., D'Orleans-Juste, P., Antunes, E., Walder, C., Warner, T. D., and Vane, J. R. (1988) Pressor effects of circulating endothelin are limited by its removal in the pulmonary circulation and by the release of prostacyclin and endothelium-derived relaxing factor. *Proc. Natl. Acad. Sci. U.S.A.* **85,** 9797–9800
32. Liu, S., Premont, R. T., Kontos, C. D., Huang, J., and Rockey, D. C. (2003) Endothelin-1 activates endothelial cell nitric-oxide synthase via heterotrimeric G-protein $\beta\gamma$ subunit signaling to protein jinase B/Akt. *J. Biol. Chem.* **278,** 49929–49935
33. Oksche, A., Boese, G., Horstmeyer, A., Furkert, J., Beyermann, M., Bienert, M., and Rosenthal, W. (2000) Late endosomal/lysosomal targeting and lack of recycling of the ligand-occupied endothelin B receptor. *Mol. Pharmacol.* **57,** 1104–1113
34. Bremnes, T., Paasche, J. D., Mehlum, A., Sandberg, C., Bremnes, B., and Attramadal, H. (2000) Regulation and intracellular trafficking pathways of the endothelin receptors. *J. Biol. Chem.* **275,** 17596–17604
35. Chun, M., Liyanage, U. K., Lisanti, M. P., and Lodish, H. F. (1994) Signal transduction of a G protein-coupled receptor in caveolae. Colocalization of endothelin and its receptor with caveolin. *Proc. Natl. Acad. Sci. U.S.A.* **91,** 11728–11732
36. Schnitzer, J. E., McIntosh, D. P., Dvorak, A. M., Liu, J., and Oh, P. (1995) Separation of caveolae from associated microdomains of GPI-anchored proteins. *Science* **269,** 1435–1439
37. Liu, J., Oh, P., Horner, T., Rogers, R. A., and Schnitzer, J. (1997) Organized endothelial cell surface signal transduction in caveolae distinct from glycosylphosphatidylinositol-anchored protein microdomains. *J. Biol. Chem.* **272,** 7211–7222
38. Oh, P., and Schnitzer, J. E. (1998) Isolation and subfractionation of plasma membranes to purify caveolae separately from glycosyl-phospatidylinositol-anchored protein microdomains. In *Cell Biology: A Laboratory Handbook* (Celis, J., ed) Academic Press, Orlando, FL
39. Rizzo, V., McIntosh, D. P., Oh, P., and Schnitzer, J. E. (1998) *In situ* flow activates endothelial nitric oxide synthase in luminal caveolae of endothelium with rapid caveolin dissociation and calmodulin association. *J. Biol. Chem.* **273,** 34724–34729
40. Schnitzer, J. E., Liu, J., and Oh, P. (1995) Endothelial caveolae have the molecular transport machinery for vesicle budding, docking, and fusion including VAMP, NSF, SNAP, annexins, and GTPases. *J. Biol. Chem.* **270,** 14399–14404
41. Oh, P., Li, Y., Yu, J., Durr, E., Krasinska, K. M., Carver, L. A., Testa, J. E., and Schnitzer, J. E. (2004) Subtractive proteomic mapping of the endothelial surface in lung and solid tumours for tissue-specific therapy. *Nature* **429,** 629–635
42. Okamoto, Y., Ninomiya, H., Miwa, S., and Masaki, T. (2000) Cholesterol oxidation switches the internalization pathway of endothelin receptor type A from caveolae to clathrin-coated pits in Chinese hamster ovary cells. *J. Biol. Chem.* **275,** 6439–6446
43. Zhang, J., Barak, L. S., Anborgh, P. H., Laporte, S. A., Caron, M. G., and Ferguson, S. S. (1999) Cellular trafficking of G protein-coupled receptor/β-arrestin endocytic complexes. *J. Biol. Chem.* **274,** 10999–11006
44. Chen, X., Berrou, J., Nguyen, G., Sraer, J. D., and Rondeau, E. (1995) Endothelin-1 induces rapid and long lasting internalization of the thrombin receptor in human glomerular epithelial cells. *Biochem. Biophys. Res. Commun.* **217,** 445–451
45. Oh, P., and Schnitzer, J. E. (1999) Immunoisolation of caveolae with high affinity antibody binding to the oligomeric caveolin cage. Toward understanding the basis of purification. *J. Biol. Chem.* **274,** 23144–23154
46. Hooper, N. M. (1999) Detergent-insoluble glycosphingolipid/cholesterol-rich membrane domains, lipid rafts and caveolae (review). *Mol. Membr Biol.* **16,** 145–156
47. Zheng, Y. Z., and Foster, L. J. (2009) Biochemical and proteomic approaches for the study of membrane microdomains. *J. Proteomics* **72,** 12–22
48. García-Cardeña, G., Oh, P., Liu, J., Schnitzer, J. E., and Sessa, W. C. (1996) Targeting of nitric oxide synthase to endothelial cell caveolae via palmitoylation. Implications for nitric oxide signaling. *Proc. Natl. Acad. Sci. U.S.A.* **93,** 6448–6453
49. Shaul, P. W., Smart, E. J., Robinson, L. J., German, Z., Yuhanna, I. S., Ying, Y., Anderson, R. G., and Michel, T. (1996) Acylation targets emdothelial nitric-oxide synthase to plasmalemmal caveolae. *J. Biol. Chem.* **271,** 6518–6522
50. Macia, E., Ehrlich, M., Massol, R., Boucrot, E., Brunner, C., and Kirchhausen, T. (2006) Dynasore, a cell-permeable inhibitor of dynamin. *Dev. Cell* **10,** 839–850
51. Newton, A. J., Kirchhausen, T., and Murthy, V. N. (2006) Inhibition of dynamin completely blocks compensatory synaptic vesicle endocytosis. *Proc. Natl. Acad. Sci. U.S.A.* **103,** 17955–17960
52. Pula, G., Mundell, S. J., Roberts, P. J., and Kelly, E. (2004) Agonist-independent internalization of metabotropic glutamate receptor 1a is arrestin- and clathrin-dependent and is suppressed by receptor inverse agonists. *J. Neurochem.* **89,** 1009–1020
53. Mukherjee, S., Ghosh, R. N., and Maxfield, F. R. (1997) Endocytosis. *Physiol. Rev.* **77,** 759–803
54. Schnitzer, J. E. (2001) Caveolae. From basic trafficking mechanisms to targeting transcytosis for tissue-specific drug and gene delivery *in vivo*. *Adv. Drug Deliv Rev.* **49,** 265–280
55. Dessy, C., Kelly, R. A., Balligand, J. L., and Feron, O. (2000) Dynamin mediates caveolar sequestration of muscarinic cholinergic receptors and alteration in NO signaling. *EMBO J.* **19,** 4272–4280
56. Stowell, M. H., Marks, B., Wigge, P., and McMahon, H. T. (1999) Nucleotide-dependent conformational changes in dynamin. Evidence for a mechanochemical molecular spring. *Nat. Cell Biol.* **1,** 27–32